# Dual energy CT in practice: Basic principles and applications

Joseph R. Grajo, MD; Manuel Patino, MD; Andrea Prochowski, MD; Dushyant V. Sahani, MD

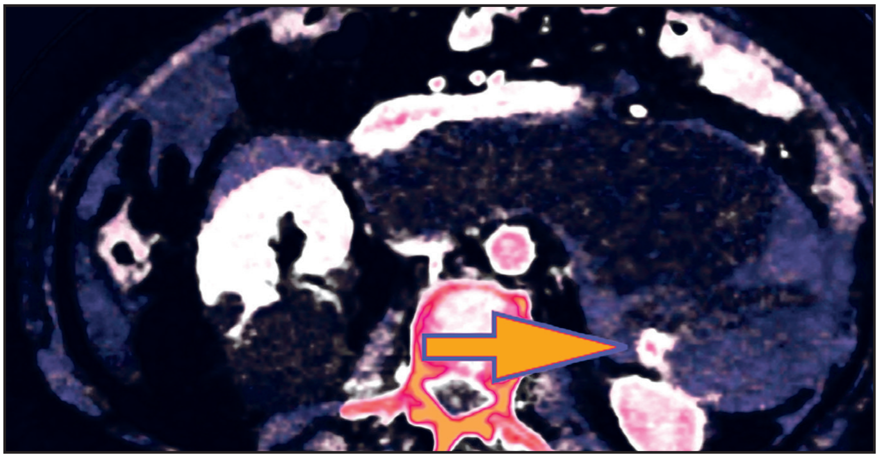

Computed tomography (CT) is the workhorse of modern medical imaging, accounting for approximately 65 million adult scans in the United States each year.[1] Technical advances such as faster scan times, thinner slices, multiplanar reformatting, and 3D rendering have revolutionized the scope of CT. An exciting development that offers great promise to further increase the modality's potential is dual energy CT (DECT). Also known as "spectral imaging," DECT was first conceptualized in the 1970s.[2-5] However, the clinical application of DECT has only recently been realized as a result of robust improvements in performance and post-processing capabilities.

Conventional or single energy CT (SECT) utilizes a single polychromatic X-ray beam (ranging from 70 to 140 kVp with a standard of 120 kVp) emitted from a single source and received by a single detector. The inherent contrast of the image dataset generated by this process depends on differences in photon attenuation of the various materials that constitute the human body (ie, soft tissue, air, calcium, fat). The degree that a material will attenuate the X-ray beam is dependent on (1) tissue composition and (2) photon energy level and how closely it exceeds the k-edge (ie, inner electron shell binding energy) of the material. Therefore, tissue attenuation can be manipulated by changing photon energy levels. In DECT, two energy levels (typically 80 and 140 kVp) are used to acquire images that can be processed to generate additional datasets.

There are currently three DECT platforms marketed by three of the major CT vendors. Dual source DECT (dsDECT) [Somatom Definition Flash, Siemens Medical Solutions, Forchheim, Germany] utilizes two X-ray tubes and two detectors to obtain simultaneous dual energy acquisition and data processing. Single source DECT (ssDECT) [Discovery 750HD, GE Healthcare, Milwaukee, WI] uses a single X-ray tube that rapidly alternates between low and high energies (fast-switching) and a single detector that quickly registers information from both energies. In detector based spectral CT [IQon spectral CT, Philips Healthcare, Eindhoven, The Netherlands], a single X-ray tube with full dose modulation capabilities is paired with a detector made of two layers (sandwich detector) that simultaneously detects two energy levels.

*Dr. Grajo is an Assistant Professor of Radiology and an Abdominal Radiologist at the University of Florida College of Medicine, Gainesville, FL; while Dr. Patino, Dr. Prochowski, and Dr. Sahani are all radiologists with the Division of Abdominal Imaging in the Department of Radiology at Massachusetts General Hospital, Harvard Medical School, Boston, MA.*

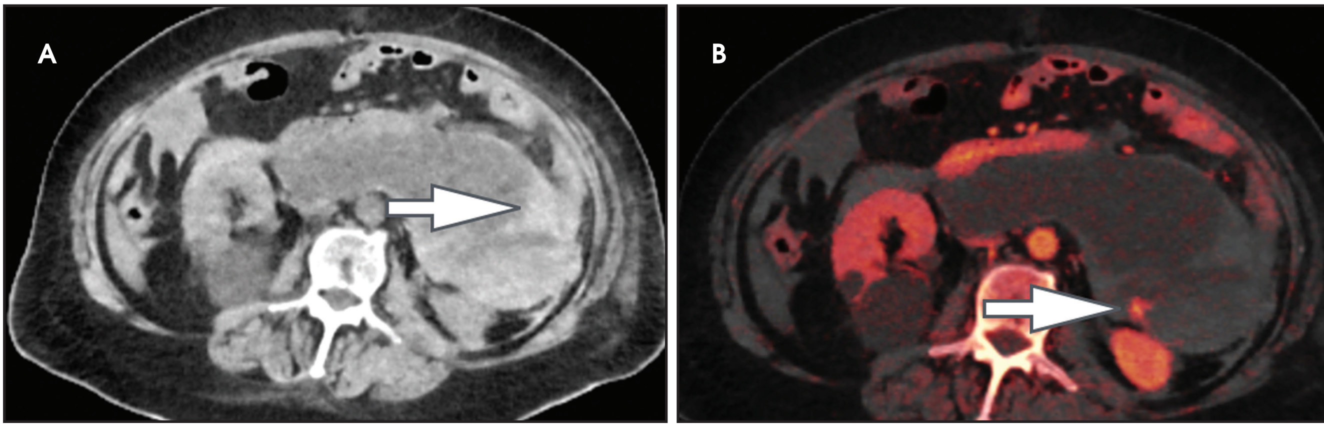


*FIGURE 1.* A 73-year-old woman who presented to the Emergency Department after a recent laparoscopic resection of a pelvic mass. (A) Dual source DECT arterial phase 60 keV virtual monochromatic image (Siemens) demonstrates a focus of active contrast extravasation (arrow). (B) Color overlay iodine material decomposition image nicely demonstrates the blush (arrow) with increased conspicuity. (C) A virtual unenhanced dataset can be generated to confirm high-density hemorrhage (arrow) without the need for a separate true unenhanced acquisition.

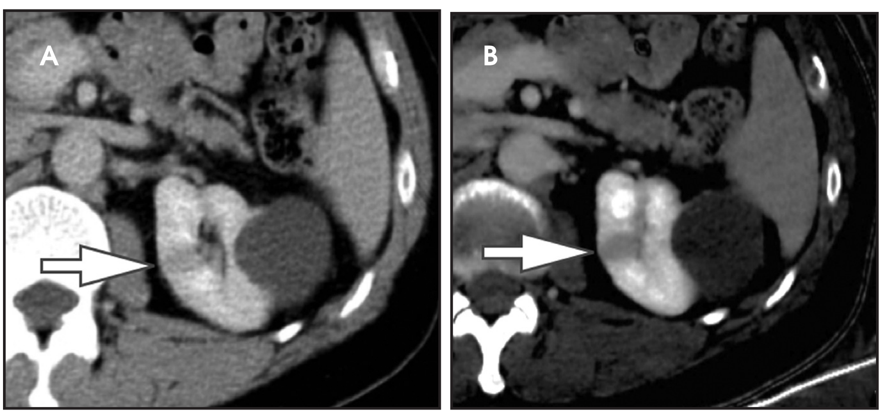


*FIGURE 2.* A 55-year-old man with hematuria. (A) Conventional CT image demonstrates a solid enhancing left renal mass (arrow) with ill-defined margins. (B) Single source DECT iodine material decomposition image (GE) better defines the margins of the tumor (arrow) due to different concentrations of iodine within the mass and surrounding parenchyma.

## Material separation

Dual energy CT offers the potential to analyze material composition through image acquisition at two different energy levels. Since materials have unique attenuation profiles at different energy levels according to their linear attenuation coefficient, DECT can utilize mathematical algorithms to examine tissues when exposed to both low and high-energy polychromatic X-ray beams. Materials with low atomic numbers (eg, water) demonstrate small differences in attenuation between high and low X-ray energies while materials with high atomic numbers (eg, iodine) show large differences in attenuation at different photon energies.

DECT scanners can process both routine diagnostic images and material decomposition (also known as material-specific or material density) images. Routine diagnostic images are intended to mirror the standard images produced by SECT. Blended images (Siemens) are created through a combination of the acquired low-energy (80 kVp) and high-energy (140 kVp) data to simulate a standard 120 kVp dataset. Virtual monochromatic (VMC) or monoenergetic (VME) [GE/Siemens] images are generated to simulate a scan obtained at a single energy level. VMC/VME images with specific energies (40 to 140 keV) provide more reliable attenuation measurements compared to polychromatic SECT. VMC images can be customized to a specific energy level for various clinical applications. Low-energy VMC images are suggested for studies with high contrast between lesions and adjacent tissues (eg, CT angiography; 45-55 keV). Intermediate-energy VMC images (60-75keV) are ideal for evaluation of soft tissues due to the balance between adequate contrast and reduced image noise. High-energy VMC images (95-140keV) reduce artifacts from metal implants.

The algorithms for material decomposition are unique for each CT manufacturer. ssDECT algorithms mathematically transform material attenuation information into the amount (or concentration) of two-material pairs that would be necessary to produce the measured attenuation level within each image voxel based on the difference of atomic numbers of the materials present within the voxel. The two-material decomposition algorithm creates material-specific image pairs, such as water and iodine images. dsDECT utilizes a three material decomposition algorithm to create soft tissue, fat, and iodine material-specific images.

Of all the possible material-specific images, iodine and water (or virtual unenhanced) images offer the most practical datasets for everyday clinical imaging (Figure 1). Iodine images demonstrate the amount of iodine (mg/ml) within an image voxel and its distribution in tissues. Because iodine images are independent of inherent tissue attenuation, they are a more reliable measure of enhancement compared to

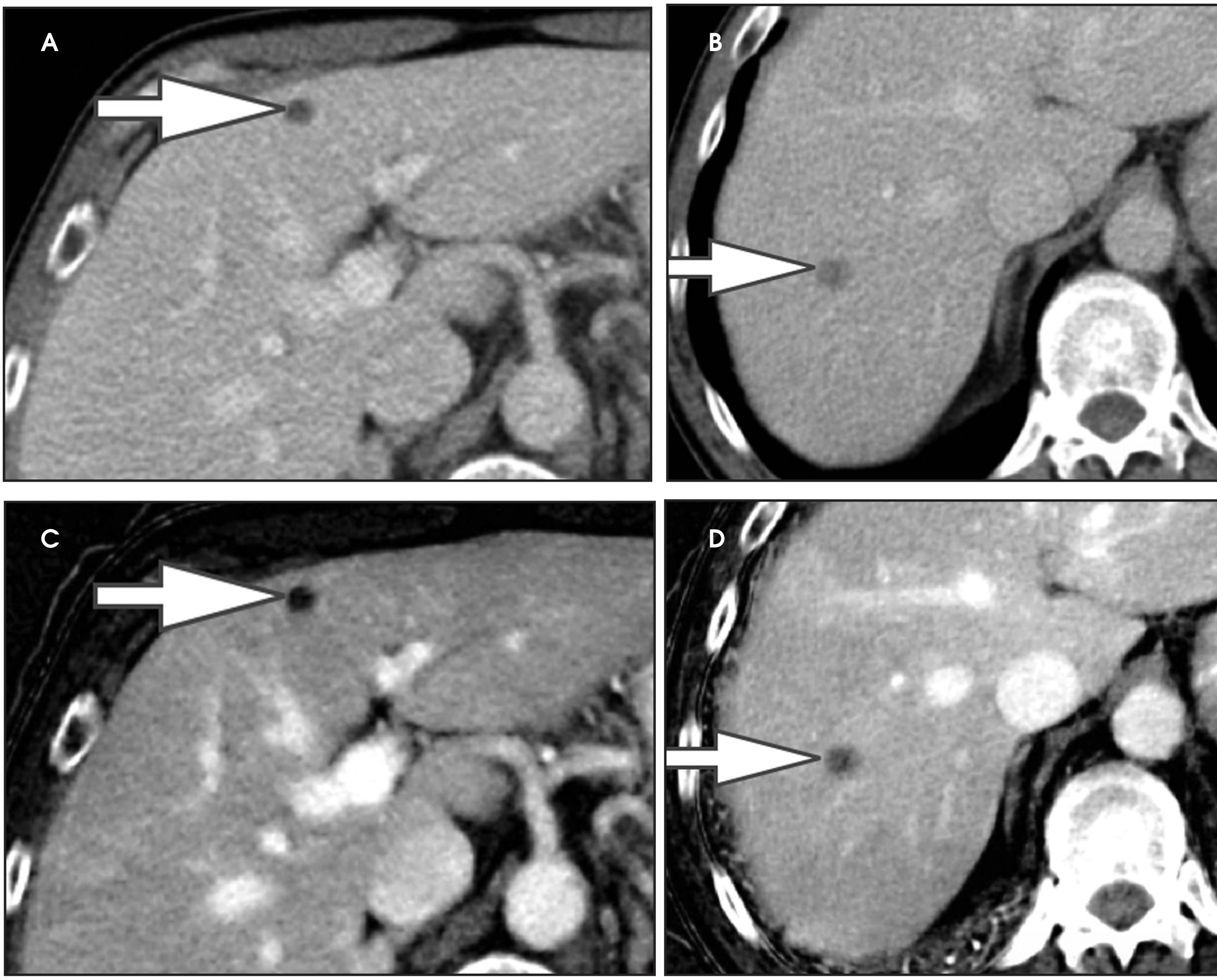


***FIGURE 3.*** *A 65-year-old man with history of colon cancer. Contrast-enhanced portal venous phase single energy CT images show two small rounded hypodense lesions in hepatic segments IV (arrow in A) and VII (arrow in B), which are very similar in appearance. Iodine material decomposition images reveal the different nature of the two lesions. the segment IV lesion demonstrates no uptake of iodine and is therefore a cyst (arrow in C), while the segment VII lesion demonstrates iodine uptake (arrow in D) and is therefore a metastasis.*

conventional contrast-enhanced studies. Water (ssDECT) or virtual unenhanced (dsDECT) images can be used to simulate true unenhanced images, therefore, possibly eliminating the need for an unenhanced acquisition altogether. This would reduce both radiation dose and exam time.

## Tissue characterization

Dual energy applications add value to CT imaging due to superior lesion detection and characterization. The single most important property that governs the interpreter's ability to detect a lesion in the background of normal tissue is contrast-to-noise ratio (CNR). The lower energy level of DECT acquisition (typically 80 kVp) improves CNR because the average photon energy is closer to the k-edge of iodine (33.2 keV) compared to a single energy polychromatic beam of 120 kVp. This results in higher X-ray absorption with improved contrast between hypervascular lesions, hypovascular lesions, and normally enhancing parenchyma.[6] VMC images (60-75 keV) can be used not only to increase CNR but also to improve overall image quality due to reduced beam hardening artifact (as a result of the elimination of very low energy photons that contribute only to image noise).[7]

Iodine images play a critical role in DECT's ability to improve lesion conspicuity. They can be displayed as quantitative gray-scale images or color overlay maps, both of which improve lesion conspicuity due to differences in iodine content between lesions and normal parenchyma (Figure 2). Iodine images detect and quantify iodine within each image voxel, allowing for detection of even a small amount of enhancement within a lesion. To illustrate improved tissue characterization, liver lesion, renal mass, and renal stone characterization will be briefly discussed. The role of DECT in oncologic imaging will also be outlined.

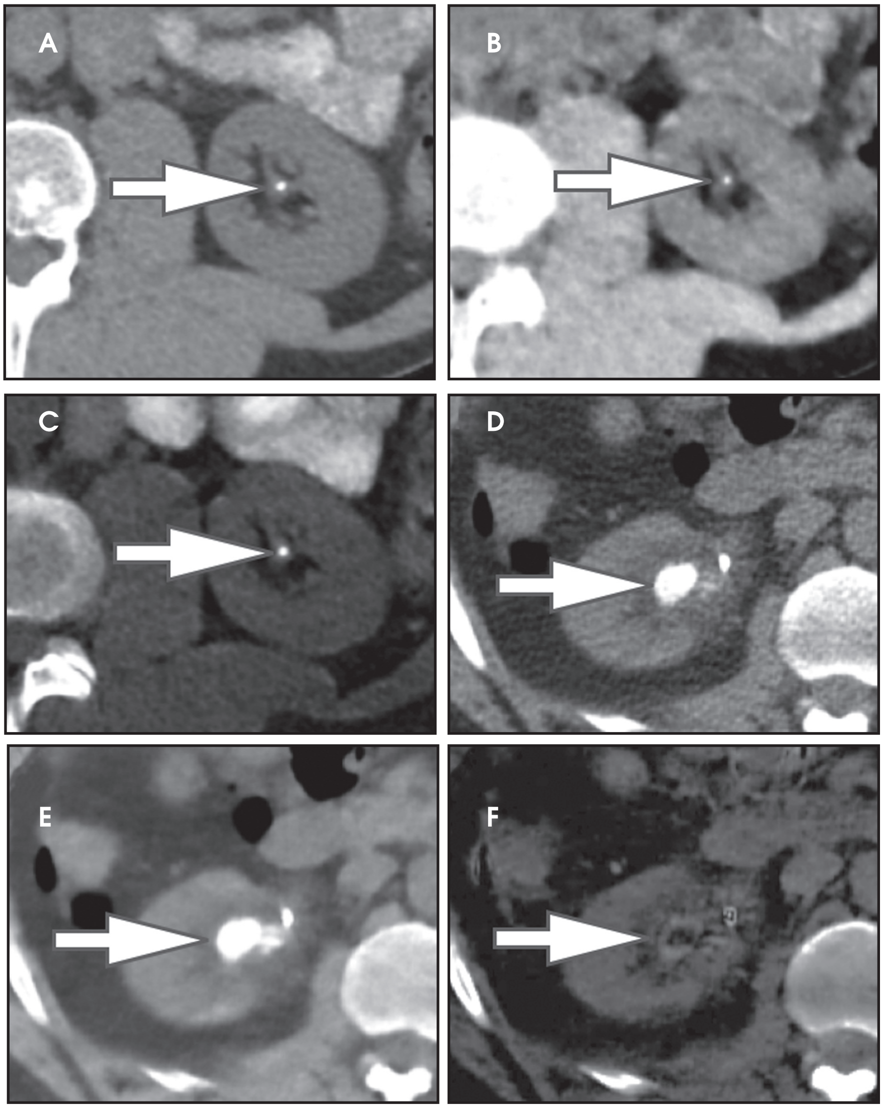


**FIGURE 4.** *45-year-old man (top row) and 60-year-old man (bottom row) with nephrolithiasis. Conventional true unenhanced image (A), water material decomposition image (B), and iodine material decomposition image (C) demonstrate a non-uric acid stone, which is hyperdense on both water and iodine images (arrows) in single source DECT (GE). In the second patient, conventional true unenhanced image (D), water image (E), and iodine image (F) demonstrate a mixed stone that is predominantly uric acid in composition (arrows). The stone is not hyperdense on iodine images except for its peripheral rim (F). Our experience has shown that uric acid stones often demonstrate a rim of calcium deposition.*

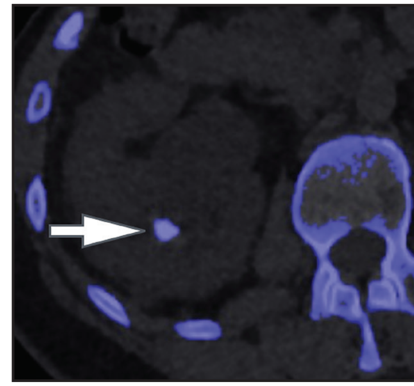

**FIGURE 5.** *A 57-year-old woman with a calcium renal stone. With dual source DECT (Siemens), calcium stones appear blue (arrow) while uric acid stones appear red.*

## *Liver lesion characterization*

Evaluation of small liver lesions on conventional CT can be a diagnostic dilemma. Subcentimeter lesions are often "too small to characterize," leading to further workup with MRI or biopsy. However, cysts can be differentiated from small hypodense masses (ie, metastases) on iodine images in a DECT acquisition because a metastasis will show iodine uptake while a cyst will not (Figure 3). Improved lesion detection and characterization by DECT could potentially reduce the need for short interval follow-up studies, decrease the number of unnecessary biopsies, and improve screening for hypervascular liver tumors in cirrhotic patients.

## *Renal mass characterization*

Differentiation of a hyperdense cyst from an enhancing renal mass is a common diagnostic challenge at single-phase CT. DECT can facilitate this challenge through the generation of virtual unenhanced (or water) and iodine images.[8-16] Hyperdense cysts will demonstrate increased attenuation on virtual unenhanced images but show no iodine content on iodine images. Conversely, renal cell carcinomas will show iodine uptake on iodine images. These two lesions with vastly different prognoses and management can easily be differentiated at DECT in a single acquisition, which offers substantially less radiation than a multiphase renal mass protocol. Virtual unenhanced images can also provide supplementary information of fat, hemorrhage, and calcification within the lesion in the same fashion as true unenhanced images.

## *Renal stone characterization*

In addition to symptoms, size, and location, the composition of renal stones is critical for appropriate clinical management. It is important for the urologist to differentiate uric acid stones (treated medically) from non-uric acid stones (treated with invasive methods like extracorporeal shockwave lithotripsy or percutaneous nephrolithotripsy). Although uric acid stones tend to have lower attenuation values than non-uric acid stones (ie, struvite, cystine, and calcium) on SECT, they may be difficult to distinguish due to overlap in attenuation values.[17]

DECT can help differentiation via analysis of underlying material composition, as uric acid stones are composed


***FIGURE 6.*** *A. 72-year-old man with history of jaundice treated with biliary stent placement. (A) Single-energy CT images, which rely on differences in Hounsfield units, show an ill-defined area of heterogeneous enhancement in the uncinate process of the pancreas (arrow). (B) Iodine material decomposition images (GE), which demonstrate the actual uptake or concentration of iodine in tissues, help to better characterize and define the extent of this hypoenhancing mass (arrow), compatible with ductal adenocarcinoma. Also note how artifact reduction in dual energy CT results in better visualization of the metal stent containing refluxed oral contrast.*

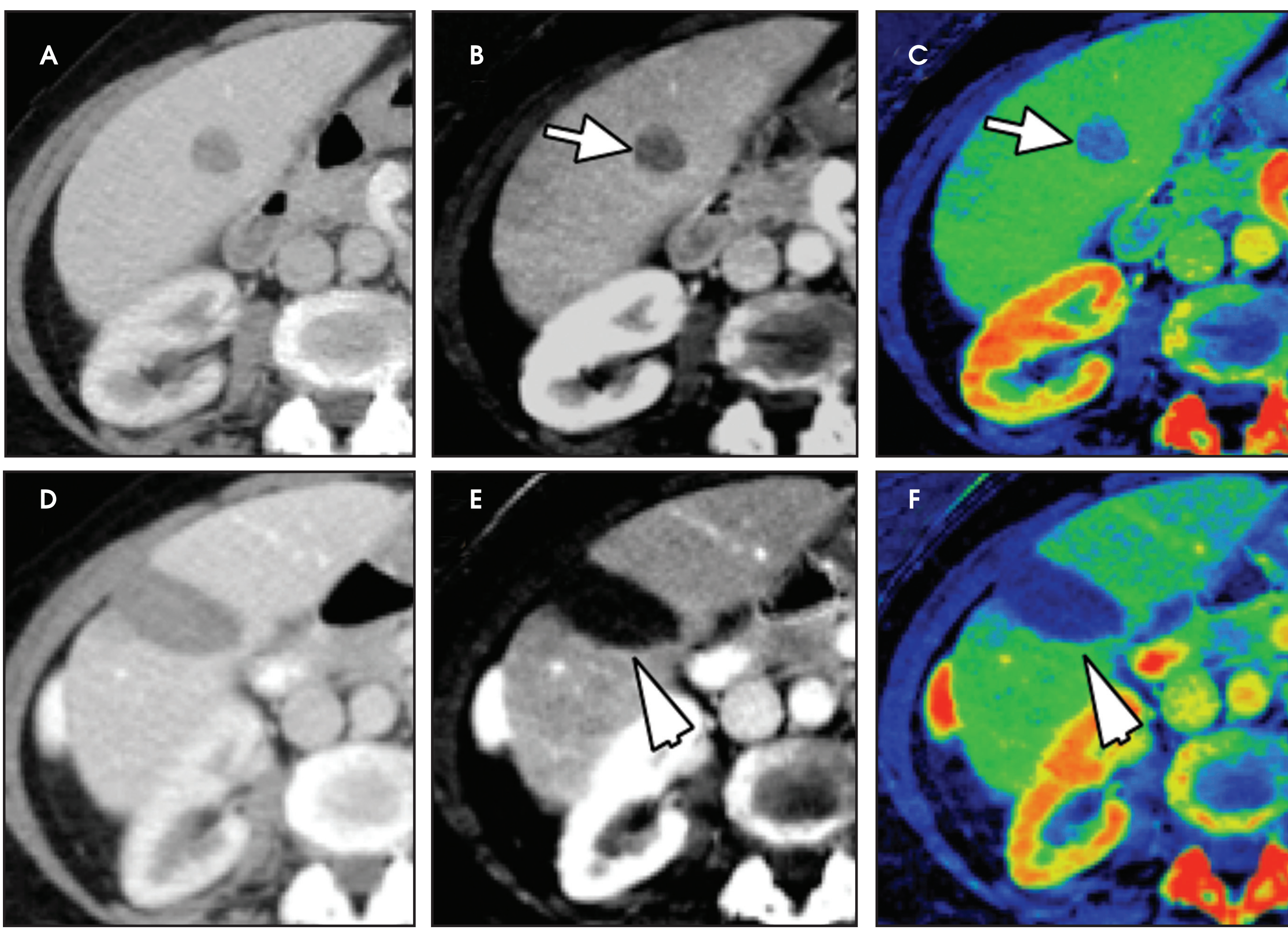


***FIGURE 7.*** *A 62-year-old woman with history of liposarcoma and a solitary liver metastasis. (A) Single energy CT image acquired at 140 kVp, (B) material decomposition iodine image, and (C) color overlay iodine image demonstrate the solitary heterogeneous liver lesion in segment V. Material decomposition iodine images (B, C) demonstrate moderate uptake of iodine (arrows), suspicious for metastasis, which was later confirmed at biopsy. Following radiofrequency ablation, the 140kVp images (D) still show heterogeneous attenuation within the metastasis, raising suspicion for incomplete ablation or recurrence. However, iodine images (E, F) show no uptake of iodine (arrowheads), excluding recurrence/incomplete ablation; the heterogeneous appearance of the lesion is likely due to post-treatment bleeding.*

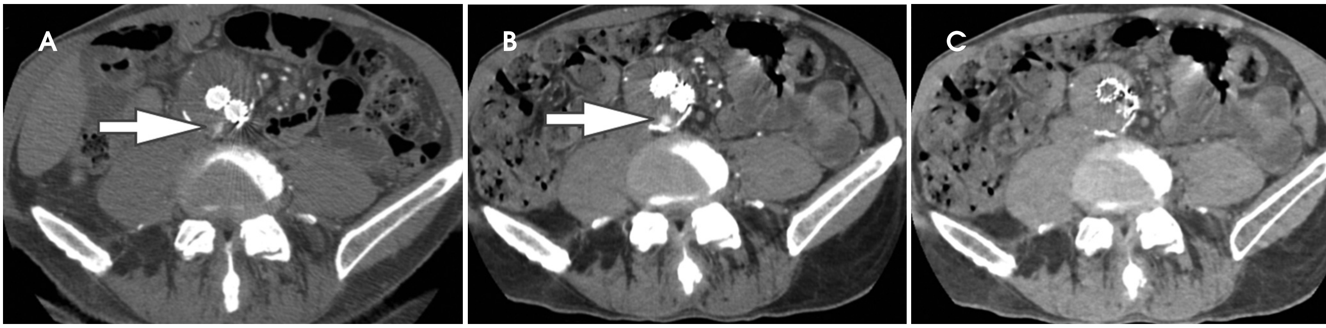


**FIGURE 8.** *A 77-year-old man with endoleak following stent graft repair of an abdominal aortic aneurysm. (A) Single energy CT at 140 kVp shows the endoleak within the aneurysm sac (arrow). (B) Follow up dual energy CT virtual monochromatic image at 65 keV with 30% reduction of IV contrast load demonstrates no loss of image quality and a more conspicuous appearance of the endoleak (arrow). Also note reduction in the degree of streak artifact from the stent graft. (C) In addition to reducing contrast load and artifact, dual energy CT also allows acquisition of virtual unenhanced images, negating the need for a separate true unenhanced acquisition.*

of lighter elements (hydrogen, carbon, oxygen, and nitrogen) while non-uric acid stones are composed of heavier elements (calcium, phosphorus, and sulfur). Uric acids stones demonstrate increased photon attenuation at 140 kVp because the attenuation is driven primarily by Compton scatter (due to lighter element chemical composition). Conversely, non-uric acid stones demonstrate increased attenuation at 80 kVp due to increased photoelectric effect contribution from the heavier elements nearing the k-edge of calcium (Z=20).

Using the two-material (basis pair) decomposition approach on ssDECT, water and iodine image datasets are generated. Stone visualization on water images only suggests uric acid calculi, whereas visualization on both water and iodine images implies non-uric acid stones (Figure 4). Effective Z ($Z_{eff}$) images are an alternative approach for renal stone characterization and can be generated in an offline workstation. $Z_{eff}$ weights both the attenuation and atomic number of certain materials, thereby facilitating the identification of predominant materials within mixed stones. Low $Z_{eff}$ is commonly seen in uric acid stones, whereas high $Z_{eff}$ is seen in non-uric acid stones.

The algorithm for kidney stones in dsDECT assumes that all voxels are a mixture of calcium, uric acid, and water. Stones with X-ray attenuation profiles similar to calcium appear blue while stones with profiles similar to uric acid appear red (Figure 5).

## Oncologic imaging

DECT has several applications in both initial and post-treatment oncologic imaging. By increasing lesion conspicuity, tumor margins are better delineated, allowing for more accurate size measurements (Figure 6). Accurate measurement on restaging examinations is important for guiding management, especially for patients in clinical trials in which tumor response is reliant on serial measurements according to Response Evaluation Criteria in Solid Tumors (RECIST) or World Health Organization (WHO) criteria, for example. DECT offers yet more potential for assessing treatment response due to the potential ability of quantitative iodine maps to evaluate and quantify tumor viability. Although this technique requires validation and standardization, it is an exciting development that may allow for characterization of tumor at a functional level that predates any change in size.[18-19]

In addition to increasing lesion conspicuity, low keV and material density images can also provide accurate delineation of locoregional extent of disease and relationships to adjacent vasculature that is useful to guide treatment planning.[18, 20] Of particular interest, iodine maps can help differentiate tumor from bland thrombus through qualitative and quantitative demonstration of iodine within the clot. This differentiation is critical in hepatocellular and renal cell carcinoma staging.

Finally, DECT can help assess response to treatment related to locoregional targeted therapies, such as ablation (eg, radiofrequency, microwave, cryo), targeted radiation therapy (eg, protons), and intra-arterial therapy (eg, selective internal radiation therapy [SIRT] and transarterial chemoembolization [TACE]). Iodine maps obtained immediately after radiofrequency ablation have shown better lesion conspicuity and internal homogeneity of the ablation zone, providing an additional benefit for assessing the safety margin after radiofrequency ablation.[21] In our practice, we have observed that iodine images are helpful not only immediately after the procedure but also for follow up of patients undergoing hepatic microwave/radiofrequency ablation and renal cryo/radiofrequency ablation (Figure 7).

## Vascular imaging

CT angiography (CTA) typically involves a multiphasic protocol with potential for higher contrast loads and radiation doses. DECT can play an important role in vascular imaging by improving image quality with less contrast and lower radiation dose compared to conventional CTA (Figure 8). Since tissues will attenuate more of the X-ray beam at photon energies closer to their k-edge, low energy DECT with customized VMC images can increase the attenuation of intravascular iodine while decreasing the administered contrast bolus. In addition, radiation dose can be significantly decreased through the utilization of virtual unenhanced images, which may eliminate the need for multiphasic imaging. These advantages of DECT can enhance CTA protocols while obtaining exquisite image quality. Such images may even be further improved by implementing calcium subtraction techniques at post-processing.[22]

## Artifact reduction

Artifact reduction is another potential benefit of DECT. Interpretation of conventional CT may be compromised in the setting of beam hardening and photon starvation artifacts related to metallic prostheses. Beam hardening commonly occurs as a result of attenuation of low energy photons within a polychromatic X-ray beam that contribute to scatter radiation and artifact but not image quality. By processing VMC images via DECT acquisition, these low energy photons are preferentially removed, eliminating their contribution to noise and artifact. Further artifact reduction can be accomplished through the application of metal artifact reduction software.[23] Artifact reduction is helpful clinically when evaluation of the pelvis is limited by beam hardening and streak artifact related to a hip prosthesis, for example. It is also invaluable in vascular imaging, where iodine images can help reduce streak artifact in the assessment for vascular patency and endoleak detection in patients who have been treated with coil and/or Onyx embolization.

## Future applications

Although the applications of DECT described in this article demonstrate exciting capabilities, the current clinical techniques only scratch the surface of the potential for material separation. Ongoing areas of active clinical research in abdominal imaging include detection and stratification of liver steatosis and fibrosis.[24] Material separation techniques can be used as a tool for electronic cleansing of the colon on CT colonography by differentiating tagged fecal materials from luminal air and air-tagging mixtures.[25] In musculoskeletal imaging, uric acid material decomposition images can help identify articular deposition of uric acid crystals (in addition to detection of uric acid renal stones). Material separation can also help detect bone marrow edema on CT to evaluate for subtle fractures in the setting of trauma or possible pathologic fracture. In neuroradiology, iodine images can be used to distinguish intracerebral hemorrhage from contrast after reperfusion therapy for acute ischemic stroke.[26] Finally, material separation through DECT may allow for development of new intravenous and oral contrast media as well as quantification of additional materials like gold, iron, copper, and zinc.

## Conclusion

Dual energy CT offers exciting applications and possibilities previously unavailable with conventional single energy CT. The potential benefits of DECT include increased lesion detection and characterization, improved oncologic staging and evaluation of treatment response, and reduced artifacts, all at comparable or even reduced radiation doses.

## References

1. Brenner DJ. Should we be concerned about the rapid increase in CT usage? *Rev Environ Health*. 2010; 25(1):63-68.
2. Chiro GD, Brooks RA, Kessler RM, et al. Tissue signatures with dual-energy computed tomography. *Radiology*. 1979; 131(2):521-523.
3. Genant HK, Boyd D. Quantitative bone mineral analysis using dual energy computed tomography. *Invest Radiol*. 1977; 12(6):545-551.
4. McDavid WD, Waggener RG, Dennis MJ, et al. Estimation of chemical composition and density from computed tomography carried out at a number of energies. *Invest Radiol*. 1977; 12(2):189-194.
5. Millner MR, McDavid WD, Waggener RG, et al. Extraction of information from CT scans at different energies. *Med Phys*. 1979; 6(1):70-71.
6. Patel BN, Thomas JV, Lockhart ME, et al. Single-source dual-energy spectral multidetector CT of pancreatic adenocarcinoma: optimization of energy level viewing significantly increases lesion contrast. *Clin Radiol*. 2013;68(2):148–154.
7. Matsumoto K, Jinzaki M, Tanami Y, et al. Virtual monochromatic spectral imaging with fast kilovoltage switching: improved image quality as compared with that obtained with conventional 120-kVp CT. *Radiology*. 2011;259(1):257–262.
8. Silva AC, Morse BG, Hara AK, et al. Dual-energy (spectral) CT: applications in abdominal imaging. *Radiographics*. 2011;31(4):1031–1046; discussion 1047–1050.
9. Brown CL, Hartman RP, Dzyubak OP, et al. Dual-energy CT iodine overlay technique for characterization of renal masses as cyst or solid: a phantom feasibility study. *Eur Radiol*. 2009;19(5):1289–1295.
10. Song KD, Kim CK, Park BK, et al. Utility of iodine overlay technique and virtual unenhanced images for the characterization of renal masses by dual-energy CT. *AJR Am J Roentgenol*. 2011;197(6): W1076–1082.
11. Chandarana H, Megibow AJ, Cohen BA, et al. Iodine quantification with dual-energy CT: phantom study and preliminary experience with renal masses. *AJR Am J Roentgenol*. 2011;196(6):W693–700.
12. Graser A, Johnson TRC, Hecht EM, et al. Dual-energy CT in patients suspected of having renal masses: can virtual nonenhanced images replace true nonenhanced images? *Radiology*. 2009;252(2):433–440.
13. Graser A, Becker CR, Staehler M, et al. Single-phase dual-energy CT allows for characterization of renal masses as benign or malignant. *Invest Radiol*. 2010;45(7):399–405.
14. Kaza RK, Caoili EM, Cohan RH, et al. Distinguishing enhancing from nonenhancing renal lesions with fast kilovoltage-switching dual-energy CT. *AJR Am J Roentgenol*. 2011;197(6):1375–1381.
15. Leschka S, Stolzmann P, Baumüller S, et al. Performance of dual-energy CT with tin filter technology for the discrimination of renal cysts and enhancing masses. *Acad Radiol*. 2010;17(4):526–534.
16. Neville AM, Gupta RT, Miller CM, et al. Detection of renal lesion enhancement with dual-energy multidetector CT. *Radiology*. 2011;259(1):173–183.
17. Kulkarni NM, Eisner BH, Pinho DF, et al. Determination of renal stone composition in phantom and patients using single-source dual-energy computed tomography. *J Comput Assist Tomogr*. 2013;37:37–45.
18. DeCecco CN, Darnell A, Rengo M, et al. Dual-energy CT: oncologic applications. *AJR Am J Roentgenol*. 2012;199(5):S98–S105.
19. Jiang T, Zhu AX, Sahani DV. Established and novel imaging biomarkers for assessing response to therapy in hepatocellular carcinoma. *J Hepatol*. 2013;58(1):169–177.
20. Marin D, Nelson RC, Barnhart H, et al. Detection of pancreatic tumors, image quality, and radiation dose during the pancreatic parenchymal phase: effect of a low-tube-voltage, high-tube-current CT technique--preliminary results. *Radiology*. 2010;256(2):450–459.
21. Lee SH, Lee JM, Kim KW, et al. Dual-energy computed tomography to assess tumor response to hepatic radiofrequency ablation: potential diagnostic value of virtual noncontrast images and iodine maps. *Invest Radiol*. 2011;46(2):77–84.
22. Coursey CA, Nelson RC, Boll DT, et al. Dual-energy multidetector CT: how does it work, what can it tell us, and when can we use it in abdominopelvic imaging? *RadioGraphics*. 2010;30(4):1037-1055.
23. Lee YH, Park KK, Song HT, et al. Metal artefact reduction in gemstone spec- tral imaging dual-energy CT with and with- out metal artefact reduction software. *Eur Radiol*. 2012;22(6):1331–1340.
24. Lamb P, Sahani D, Fuentes-Orrego J, et al. Stratification of patients with liver fibrosis using Dual-Energy CT. *IEEE Trans Med Imaging*. 2014 Aug 28 [Epub ahead of print].
25. Cai W, Kim SH, Lee JG, et al. Informatics in radiology: dual-energy electronic cleansing for fecal-tagging CT colonography. *RadioGraphics*. 2013;33(3):891-912.
26. Gupta R, Phan CM, Leidecker C, et al. Evaluation of dual-energy CT for differentiating intracerebral hemorrhage from iodinated contrast material staining. *Radiology*. 2010;257(1):205-211.